Solubility phenomena involving CaSO$_4$ in hydrometallurgical processes concerning heavy metals*

Dewen Zeng‡ and Wenlei Wang

College of Chemistry and Chemical Engineering, Central South University, 410083 Changsha, China

Abstract: Deposit of CaSO$_4$ in hydrometallurgical processes involving heavy metals usually decreases production quality and harms the production process. To avoid its formation at false time and sites, a sound understanding of the solubility behavior of CaSO$_4$ in the quaternary systems CaSO$_4$ + H$_2$SO$_4$ + (heavy metal)SO$_4$ + H$_2$O over large ranges of temperature and concentration is a prerequisite. Up to now, although a large amount of solubility data has been reported in these systems, little information is available on the solubility of anhydrite, especially at salt concentrations near saturation points. In this paper, we introduce the effect of CaSO$_4$ in hydrometallurgical processes involving heavy metals, review published solubility data of calcium sulfate and its hydrate in relevant systems, and report our newly determined solubility results involving anhydrite in the quaternary systems CaSO$_4$ + H$_2$SO$_4$ + MSO$_4$ + H$_2$O (M = Cu,Zn,Mn) at 348.1 and 363.1 K. Based on the newly obtained data some application examples were given. On account of the complexity of the solubility phase diagram of these quaternary systems, where the calcium sulfate solubility is a function of its crystal type, temperature, compositions of sulfuric acid, and heavy metal sulfate, a complete solubility phase diagram is not available until some basic data measurement, for instance, water activity at temperatures higher than 298 K, and final modeling has been finished.

Keywords: calcium sulfate; copper sulfate; hydrometallurgy; nickel sulfate; manganese sulfate; solubility.

INTRODUCTION

The abundance of calcium, with 4−5 % in mass, ranks fifth among all elements in the earth's crust, several thousands times higher than that of common heavy metals. Consequently, it exists widely in heavy metal ores or in natural water systems. Inevitably, the calcium is present in industrial electrolyte solutions. In hydrometallurgical processes, a sulfate solution is the most common medium. Unlike most heavy metal sulfates, calcium sulfate and its hydrates are slightly soluble in water, their solubilities decrease or increase with increasing temperature, depending on their hydrate types. In sulfuric acid solution, when the solubility of all heavy metal sulfates decreases with increasing sulfuric acid concentration, the solubility of calcium sulfate and its hydrates, however, increases at first and then decreases. The complicated solubility behavior of calcium sulfate makes it difficult to understand its

---

formation in complicated hydrometallurgical processes involving heavy metals. The complexities are complicated by large variations of temperature and compositions of electrolyte. For instance, in zinc hydrometallurgical process, sulfuric acid and zinc contents in the electrolyte change from 10 and 200 g L^{-1} in the leaching stage to 200 and 50 g L^{-1} in waste electrolyte, respectively. Meanwhile, the temperature changes from ~363 K in the leaching stage to 313 K in electrowinning cells. In heavy metal sulfate salt production by the vaporation-crystallization method, the salt concentration in the electrolyte increases as the solution volume decreases, and then decreases with decreasing temperature. The arbitrary formation of calcium sulfate harms the production process and affects crystal production adversely. For example, the deposition of gypsum on the walls of pipes and in filtration cloths during the electrolyte purification badly affects industrial operation conditions. In most heavy metal sulfate salt products for battery manufacture or electroplating, there are strict limitations for calcium contents; the calcium content in $CuSO_4 \cdot 5H_2O$ for electroplating should be lower than 0.0005 % in mass, and that in $NiSO_4 \cdot 6H_2O$ and $MnSO_4 \cdot H_2O$ for battery production lower than 0.01 % in mass. Control of calcium in these products becomes the most difficult task in their purification.

Theoretically, if the solubility behavior of calcium sulfate in the heavy metal sulfate systems $CaSO_4 \cdot nH_2O + MSO_4 + H_2SO_4 + H_2O$ is completely known, a series of economical approaches can be developed to avoid calcium sulfate formation when it is not wanted or to induce its formation at some other time. Unfortunately, although large numbers of solubility data for calcium sulfate and its hydrates in the above-mentioned systems have been reported, complete solubility phase diagrams are still to be developed.

AVAILABLE SOLUBILITY DATA IN THE SYSTEMS $CaSO_4$ + (HEAVY METAL)SO_4 + H_2SO_4 + H_2O

$CaSO_4$ + H_2O system

Freyer and Voigt [1] have critically evaluated some of the available solubility data [2–14] of the binary $CaSO_4 + H_2O$ system, where three crystal types exist, namely, gypsum, hemihydrate, and anhydrite. Among them, the hemihydrate is unstable in the temperature range 273–473 K. In pure water, the solubility of gypsum is relatively constant at ~0.015 mol kg^{-1} in the temperature range 273–373 K, but the solubility of anhydrite decreases with increasing temperature. Generally, gypsum is stable at lower temperatures and anhydrite at higher temperatures with the conversion point at about 315 K. At 373 K, the solubility of anhydrite is only one-third that for gypsum. For this binary system the available experimental data can be considered complete. In multicomponent systems containing sulfuric acid and heavy metal sulfate, the solubility behavior of calcium sulfate and its hydrates could be quite different from that in the binary $CaSO_4 + H_2O$ system.

$CaSO_4$ + H_2SO_4 + H_2O system

There are a large number of reports [15–20] concerning the solubility of calcium sulfate in its three hydrates in the $CaSO_4 + H_2SO_4 + H_2O$ system, as shown in Figs. 1–3.

Although there are some slight disagreements, the solubility curves of gypsum generally show the same tendency at each temperature; it rises and then falls with increasing H_2SO_4 content. In the presence of sulfuric acid, the solubility of gypsum is influenced by temperature more obviously than in the $CaSO_4 + H_2O$ system, increasing monotonously with temperature. In 1.5 mol kg^{-1} H_2SO_4 solution, the solubility of gypsum at 368 K is 4 times higher that at 298 K. In sulfuric acid solution, one can prevent the formation of gypsum by increasing temperature.
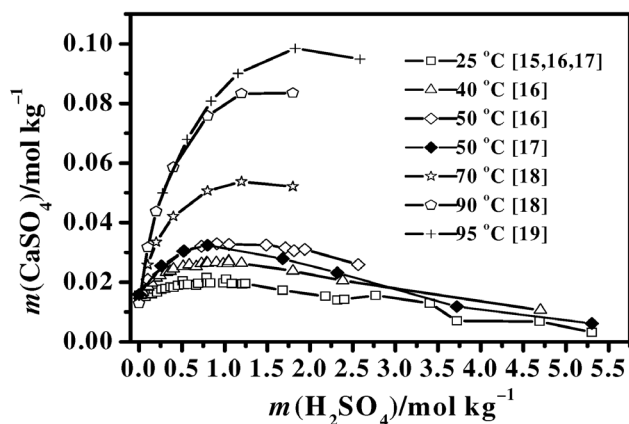
Fig. 1 Solubility of $CaSO_4 \cdot 2H_2O$ in the $CaSO_4 + H_2SO_4 + H_2O$ system [15–19].
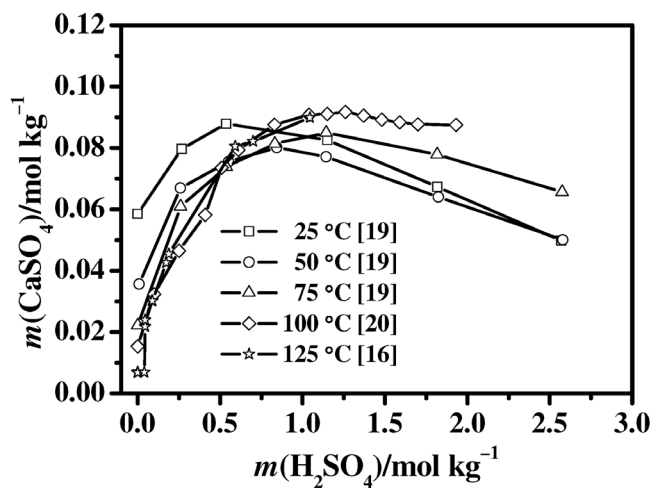
Fig. 2 Solubility of $CaSO_4 \cdot 0.5H_2O$ in the $CaSO_4 + H_2SO_4$ system $+ H_2O$ [16,19,20].

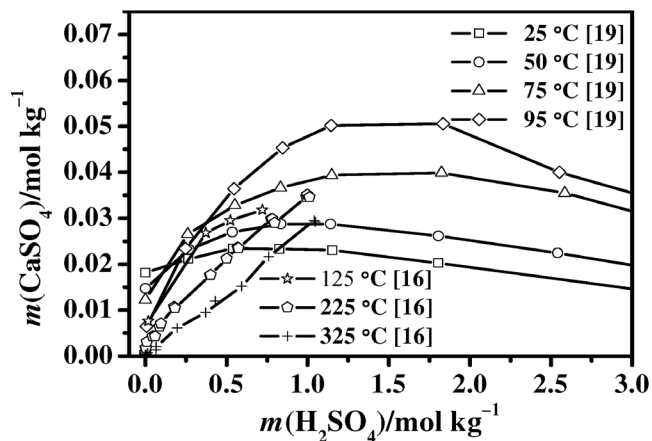**Fig. 3** Solubility of $CaSO_4$ in the $CaSO_4 + H_2SO_4 + H_2O$ system [16,19].

At constant temperature, the sulfuric acid concentration has the same influence on the solubility of hemihydrate as for gypsum. Since the solubility of hemihydrate decreases monotonously with increasing temperature in the binary $CaSO_4 + H_2O$ system, and inversely at high H_2SO_4 concentrations, the solubility representation seems a challenge for thermodynamic models [21].

As in the $CaSO_4 + H_2O$ system, solubility of anhydrite is generally lower than gypsum and hemihydrate in sulfuric acid solutions. All solubility curves for the three hydrates are convex with increasing of sulfuric acid concentrations, and this may mean that the solubilities of $CaSO_4 \cdot 2H_2O$, $CaSO_4 \cdot 0.5H_2O$, and $CaSO_4$ are mainly controlled by the influence of H_2SO_4 concentrations on the activities of Ca^{2+} and SO_4^{2-}.

$CaSO_4 + CuSO_4 + H_2SO_4 + H_2O$ system

Most of the reported solubility data [22–27] for the $CaSO_4 + CuSO_4 + H_2O$ system concerns gypsum (Fig. 4). The early experimental data [22–23] could be less reliable because of the analytical method employed. Later solubility data [25–27] for gypsum were determined by volumetric analysis, and atomic absorption spectroscopy may also be unreliable. Wollmann and Voigt [24] applied inductively coupled plasma–optical emission spectroscopy (ICP–OES) to analyze calcium contents and set the equilibrium time from 11 to 50 d, and their reported solubility data for gypsum at 298.15 and 313.15 K could be the most reliable. It was shown that gypsum solubility in $CuSO_4$ solutions decreases along with temperature, which enables us to understand why calcium sulfate will crystallize along with the product $CuSO_4 \cdot 5H_2O$ when temperature decreases. To avoid formation of gypsum during $CuSO_4 \cdot 5H_2O$ crystallization, one should keep the calcium content in the solution at quite a low level. However, no solubility data in $CuSO_4$ solutions for $CaSO_4 \cdot 2H_2O$, $CaSO_4 \cdot 0.5H_2O$, or $CaSO_4$ are reported at higher temperatures. An interesting point concerns whether the solubility behavior of anhydrite in $CuSO_4$ solution keeps its character as in pure water, at a quite lower level. The answer will not be known until we measure the solubility of anhydrite in $CuSO_4$ solutions at higher temperatures.
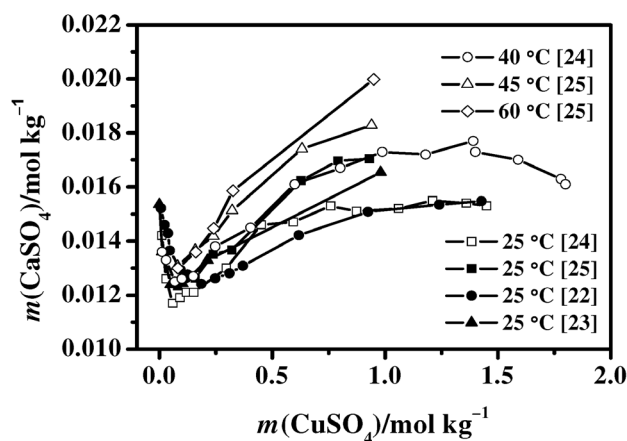

Fig. 4 Solubility of gypsum $CaSO_4 \cdot 2H_2O$ in the $CaSO_4 + CuSO_4 + H_2O$ system [22−25].

Dutrizac and Kuiper [28] studied the solubility behavior of gypsum and anhydrite in quite typical Cu-electrolyte solutions in the temperature range 298–368 K, as shown in Figs. 5 and 6. At constant copper sulfate content (0.7 mol L^{-1}), the solubility curves of gypsum are convex with increasing of sulfuric acid content. At higher temperatures, the influence of temperature on gypsum solubility gets stronger. Generally, the solubility of anhydrite is lower than that of gypsum at temperatures higher than
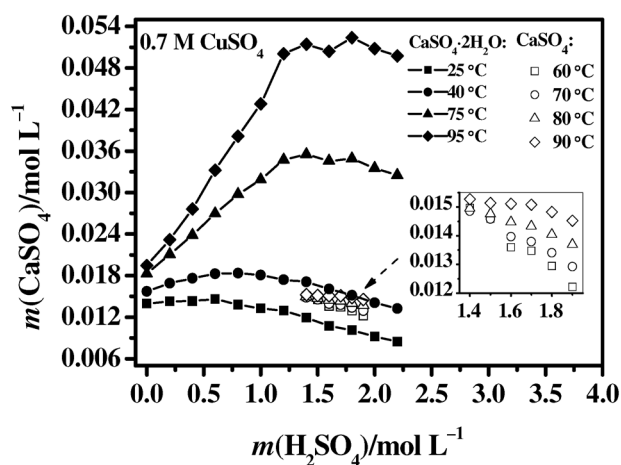
Fig. 5 Solubility of gypsum and anhydrite in the $CaSO_4$ + $CuSO_4$(0.7 M) + H_2SO_4 + H_2O system [28].
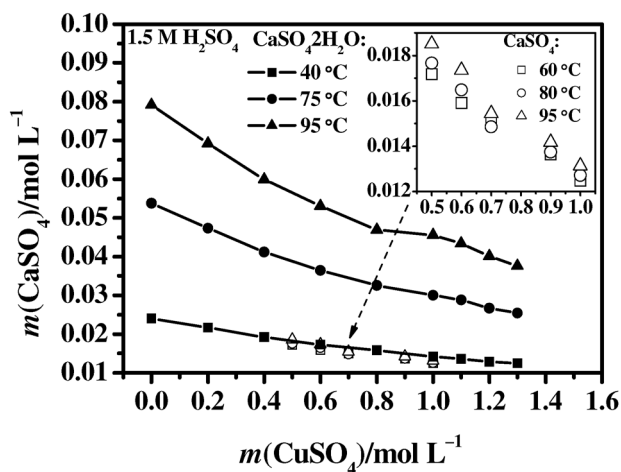
Fig. 6 Solubility of gypsum and anhydrite in the $CaSO_4$ + H_2SO_4(1.5 M) + $CuSO_4$ + H_2O system [28].

313 K. At constant H_2SO_4 (1.5 mol L^{-1}), the solubility of both gypsum and anhydrite decreases with increasing copper sulfate concentrations. In the $CuSO_4$ range 0.5–1.0 mol L^{-1}, the solubilities of anhydrite and gypsum are almost identical at about 313 K.

However, what is met in the evaporation process is $CuSO_4$ contents as high as 4–5 mol kg^{-1} and the H_2SO_4 content much lower than 1.8 mol kg^{-1}. Solubilities of gypsum and anhydrite under these conditions are unknown.

$CaSO_4$ + $ZnSO_4$ + H_2SO_4 + H_2O system

A good deal of gypsum solubility data [24,26,27,29,30] has been reported in the ternary $CaSO_4$ + $ZnSO_4$ + H_2O system (see Fig. 7). In quite concentrated $ZnSO_4$ solutions, gypsum solubility decreases to quite a low level. Unfortunately, no solubility data are reported for anhydrite.
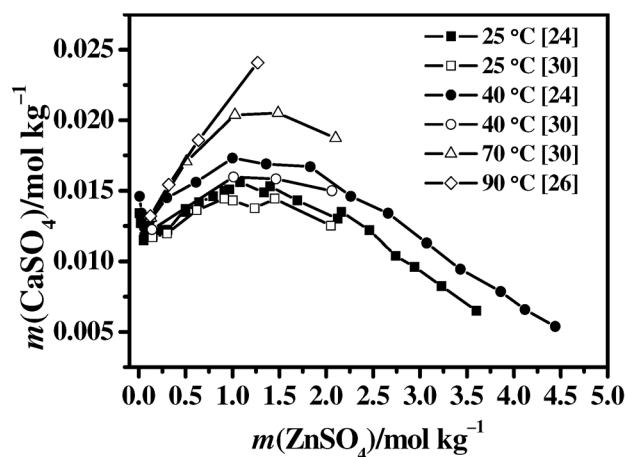
Fig. 7 Solubility of gypsum in the $CaSO_4$ + $ZnSO_4$ + H_2O system [24,26,30].

Although Dutrizac [18,31] has reported gypsum solubility in the $CaSO_4$ + $ZnSO_4$ + H_2SO_4 + H_2O system over a wide temperature range from 298 to 368 K, experiments were limited to constant $ZnSO_4$ concentrations (1.5 mol L^{-1}) or a H_2SO_4 concentration of (0.1 mol L^{-1}) (see Figs. 8 and 9). At other $ZnSO_4$ or H_2SO_4 concentrations, no solubility results for gypsum or anhydrite have been reported.
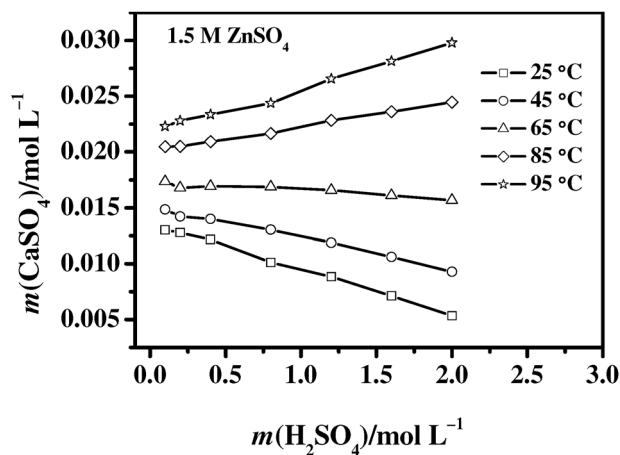

Fig. 8 Gypsum solubility in the $CaSO_4$ + $ZnSO_4$(1.5 M) + H_2SO_4+H_2O system [18].
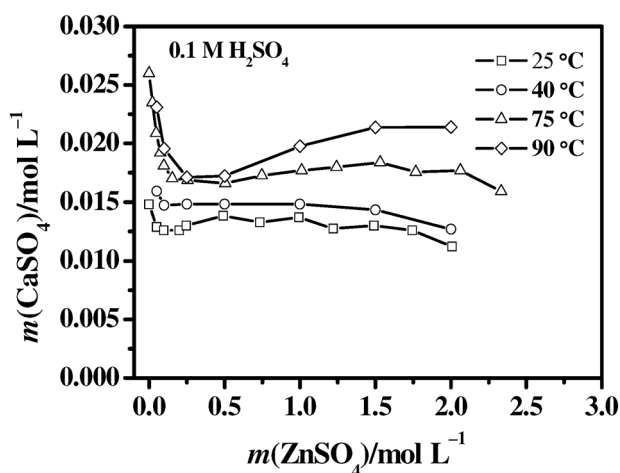
Fig. 9 Gypsum solubility in the $CaSO_4$ + H_2SO_4(0.1 M) + $ZnSO_4$ + H_2O system [18].

$CaSO_4$ + $MnSO_4$ + H_2SO_4 + H_2O system

Several research groups [24,32–34] have reported the solubility of gypsum in aqueous $MnSO_4$ solution, as shown in Fig. 10. Wollmann and Voigt's data [24] agree with Zhelnin et al. [33] and Farrah et al. [34] quite well, but differ from those reported by Korf and Fomina [32]. The $MnSO_4$ content has the same influence on the solubility of gypsum as $CuSO_4$ and $ZnSO_4$, reflecting the fact that they have a common interaction mechanism.
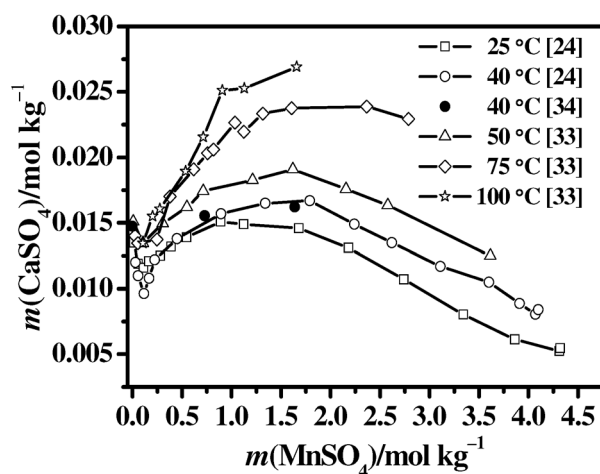

Fig. 10 Gypsum solubility in the $CaSO_4$ + $MnSO_4$ + H_2O system [24,33,34].

Farrah et al. [34] reported limited solubility data for gypsum and anhydrite in the quaternary $CaSO_4$ + $MnSO_4$ + H_2SO_4 + H_2O system, as shown in Figs. 11 and 12. However, it is not clear what the solubilities of gypsum and anhydrite are in solution with Mn^{2+} and H_2SO_4 concentrations higher than 72 g kg^{-1} of solution, since the saturated Mn^{2+} concentration is as high as ~144 g kg^{-1} of solution at 30 °C. While Zdanovskii and Vlasov [19] reported that the solubility of anhydrite increases with

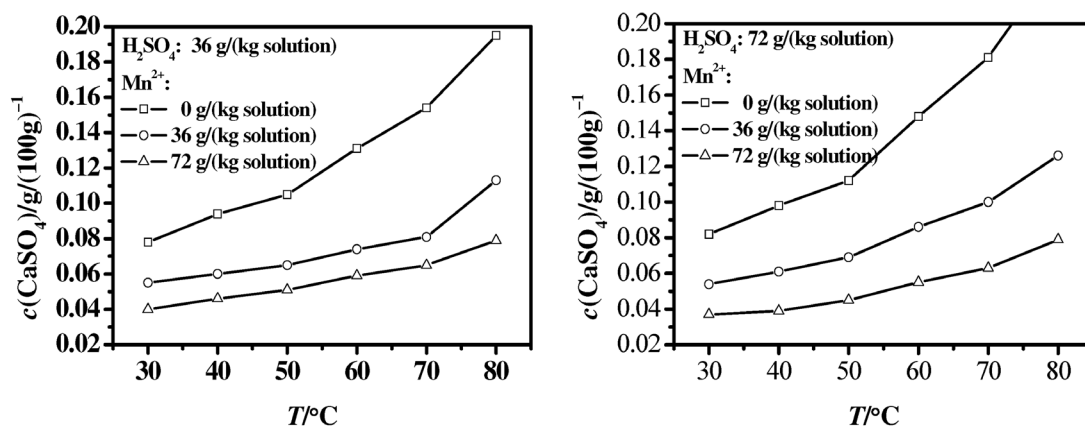**Fig. 11** Solubility of gypsum in the $CaSO_4$ + $MnSO_4$ + H_2SO_4 + H_2O system [34].
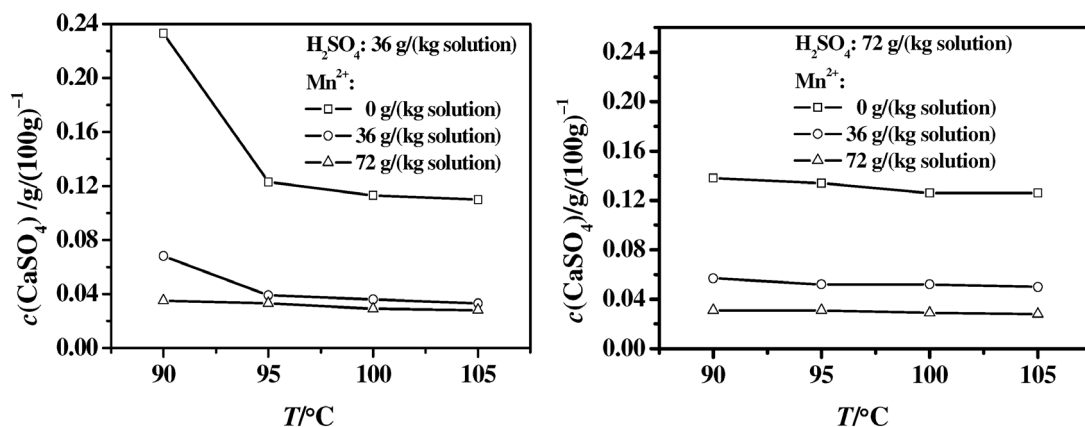
Fig. 12 Solubility of anhydrite in the $CaSO_4$ + $MnSO_4$ + H_2SO_4 + H_2O system [34].

increasing H_2SO_4 concentrations in the temperature range 298–368 K and concentration range 0.3–0.8 mol kg^{-1}, Farrah et al. [34] reported the inverse, as shown in Fig. 12, and the solubility data are in some doubt.

$CaSO_4$ + $NiSO_4$ + H_2SO_4 + H_2O system

There are many solubility reports [24,35,36] for gypsum in the $CaSO_4$ + $NiSO_4$ + H_2O system, as shown in Fig. 13. Wollmann and Voigt [24] and Azimi [36] used the same ICP–OES method for Ca analysis, and their experimental results agree quite well at 25 °C. Data from different authors [35,36] at higher temperatures deviate from each other quite significantly, the volumetrically determined data [35] may be less reliable. However, whether a 4–6 h equilibration time [36] between solid $CaSO_4·2H_2O$ and solution at high temperatures is enough should be checked further.

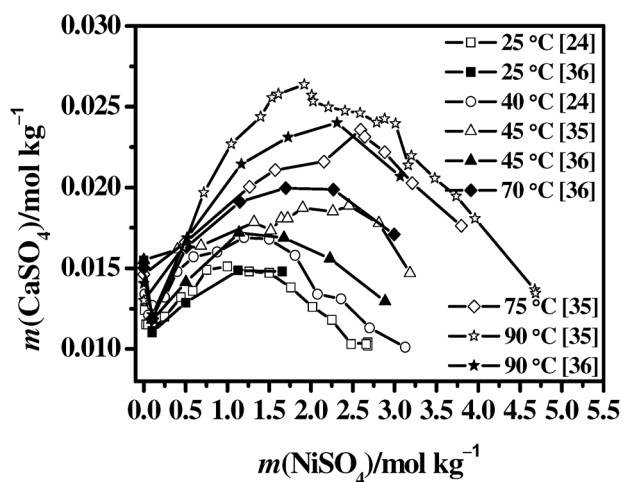**Fig. 13** Gypsum solubility in the $CaSO_4$ + $NiSO_4$ + H_2O system [24,35,36].

While Azimi and Papangelakis [36] reported the solubility of anhydrite in the $CaSO_4$ + $NiSO_4$ + H_2O system at 150 and 175 °C (see Fig. 14), data near 100 °C are still unknown, and they are necessary for control of the purification process by crystallization.
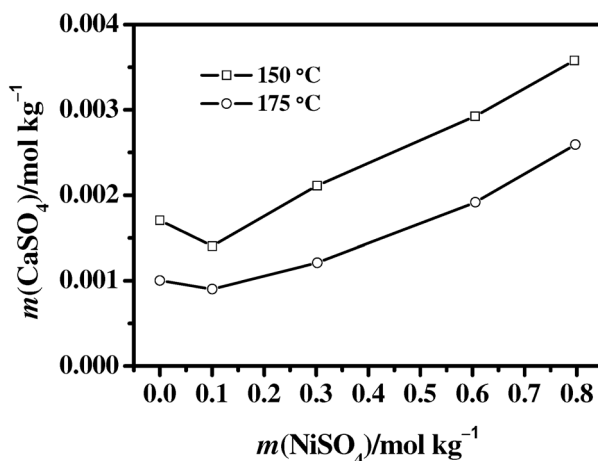

Fig. 14 Solubility of anhydrite in the $CaSO_4$ + $NiSO_4$ + H_2O system [36].

Azimi and Papangelakis [37] reported the solubility of gypsum in the $CaSO_4$ + $NiSO_4$ + H_2SO_4 system (0.5 mol kg^{-1}) + H_2O in the temperature range 20–95 °C (see Fig. 15). In solutions with H_2SO_4 concentrations other than 0.5 mol kg^{-1}, solubility data for gypsum are unknown.
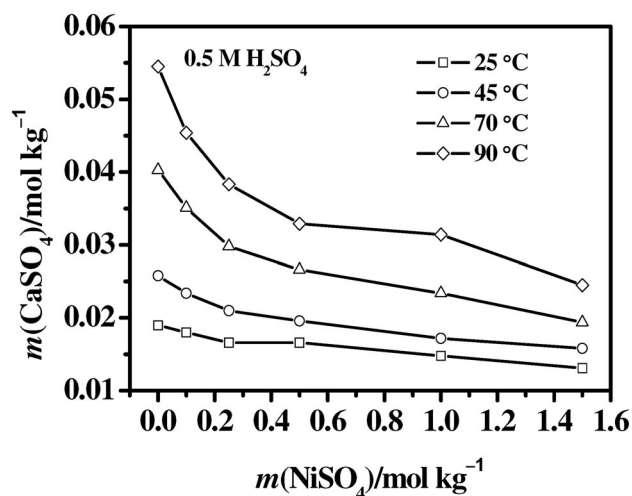
Fig. 15 Solubility of gypsum in the quaternary $CaSO_4 + NiSO_4 + H_2SO_4(0.5\ mol\ kg^{-1}) + H_2O$ system [37].

EXPERIMENTAL

Based on the above discussion, it is evident that solubility data for anhydrite are lacking in the quaternary $CaSO_4 + MSO_4 + H_2SO_4 + H_2O$ system. Therefore, we initiated a series of experimental measurements on the solubility of anhydrite in these systems.

Electrolyte solutions of $CuSO_4$, $ZnSO_4$, and $MnSO_4$ were prepared by dissolving with electrolytic metals purities higher than 99.99 % in H_2O_2 aqueous solution. The solution was reduced in volume and products crystallized four times to produce $CuSO_4 \cdot 5H_2O$, $ZnSO_4 \cdot 6H_2O$, and $MnSO_4 \cdot H_2O$. $CaSO_4 \cdot 2H_2O$ was prepared by reacting $CaCO_3$ (purity higher than 99.9 % in mass) with H_2SO_4 and recrystallizing the product several times. H_2SO_4 had a purity higher than 99.9 % in mass.

Heavy metal sulfate contents were determined by precipitating SO_4^{2-} using $BaCl_2$. Ca^{2+} was analyzed by ICP, where different amounts of known Ca solutions were added to the sample solution and the initial Ca^{2+} content determined. The analysis error for Ca^{2+} and heavy metal sulfate could be controlled to within 2 and 0.1 %, respectively.

Equilibrium experiments were carried using a Lauda E219 with a temperature stability of ±0.05 K and an accuracy of ±0.1 K.

To determine the equilibrium time needed, we began an experiment involving anhydrite with both supersaturated and undersaturated solutions, respectively, and measured the Ca^{2+} concentration with time, as shown in Fig. 16. It is noted that the undersaturated solution reaches equilibrium faster than the supersaturated solution and that 100 h equilibration time is enough at both 348 and 363 K. In subsequent experiments, the undersaturated solution was always used and the equilibration time set to 5 days, or about 120 h. At the end of each experiment, the solution was left to stand unstirred for 8 h and then the supernatent sampled in a weighed tube and analyzed by the methods described above.
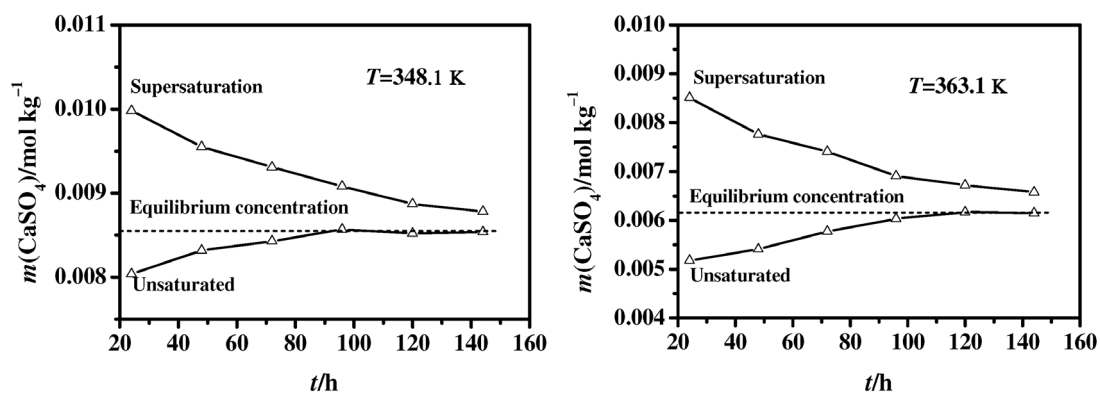
Fig. 16 Ca^{2+} concentration as a function of equilibrium time in the aqueous $CaSO_4$ solution in contact with anhydrite.

EXPERIMENTAL RESULTS

Measured solubility data for anhydrite in the $CaSO_4 + H_2SO_4 + MSO_4 + H_2O$ system at 348.1 and 363.1 K are presented in Figs. 17–19 and listed in Tables 1–6 in the Supplementary Information for this paper. Generally, in sulfuric acid-free solutions in all cases, the $CaSO_4$ concentration decreases at first, increases after reaching a minimum, and then decreases with increasing concentrations of heavy metal sulfate, something like the solubility isotherms of gypsum at lower temperatures [24].
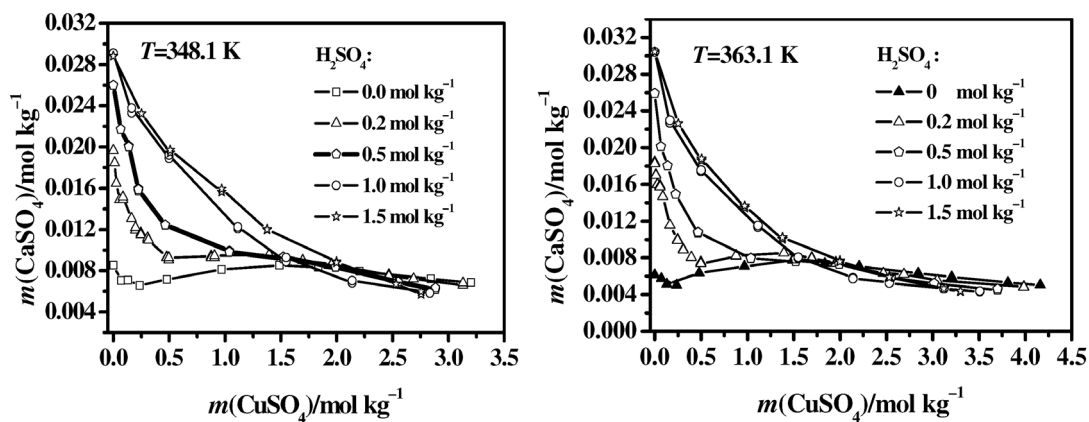

Fig. 17 Solubility of anhydrite in the $CaSO_4 + H_2SO_4 + CuSO_4 + H_2O$ system at 348.1 and 363.1 K.
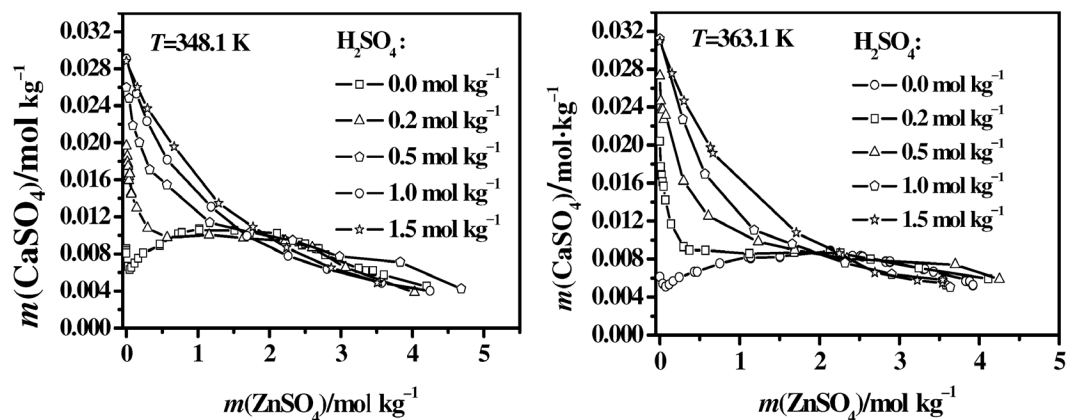
Fig. 18 Solubility of anhydrite in the $CaSO_4 + H_2SO_4 + ZnSO_4 + H_2O$ system at 348.1 and 363.1 K.
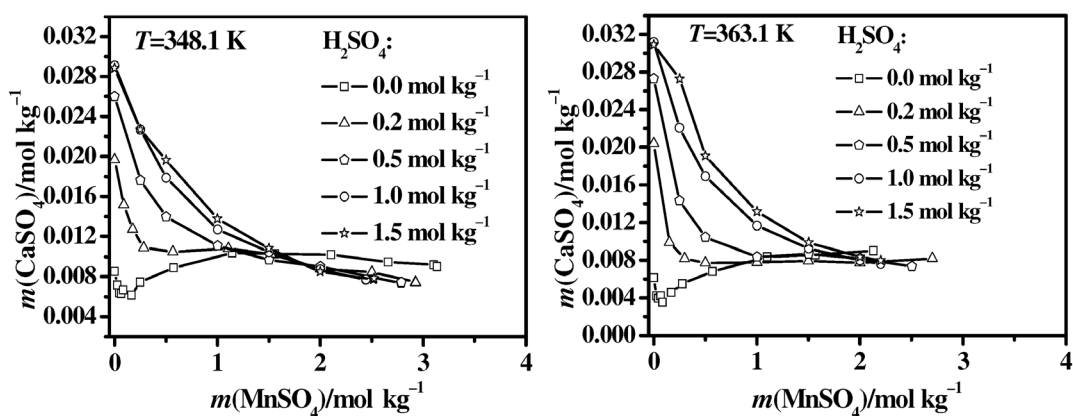
Fig. 19 Solubility of anhydrite in the $CaSO_4 + H_2SO_4 + MnSO_4 + H_2O$ system at 348.1 and 363.1 K.

In pure aqueous H_2SO_4 solutions, our experimental solubility data for anhydrite at 348.1 and 363.1 K are systematically lower than the literature data [19] (see Fig. 20). It is of interest to know which experimental data are more reliable. We note that solubility data for anhydrite predicted by Azimi et al. [21] using an MSE model are also systematically lower than the literature data [19] but agree with our data. We also note that the equilibrium time used in the literature [19] is only 5–6 h, which is very likely too short. Farrah et al.'s [34] solubility data for anhydrite are quite different from the literature data [19] and our data, and may represent metastable data conditions.

When sulfuric acid concentration is higher than 0.5 mol kg^{-1}, anhydrite solubility decreases monotonously with increasing concentrations of heavy metal sulfate (see Figs. 17–19). It is noted that the solubility of anhydrite increases with increasing temperature in pure aqueous H_2SO_4 solutions (>0.3 mol kg^{-1}), but decreases in mixed heavy metal sulfate and sulfuric acid solutions, as shown in Fig. 21.
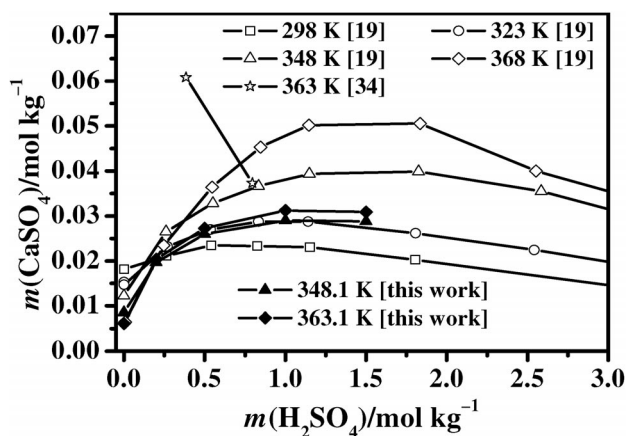
Fig. 20 Solubility data for anhydrite in aqueous H_2SO_4 solutions in this work and comparison with literature data [19,34].
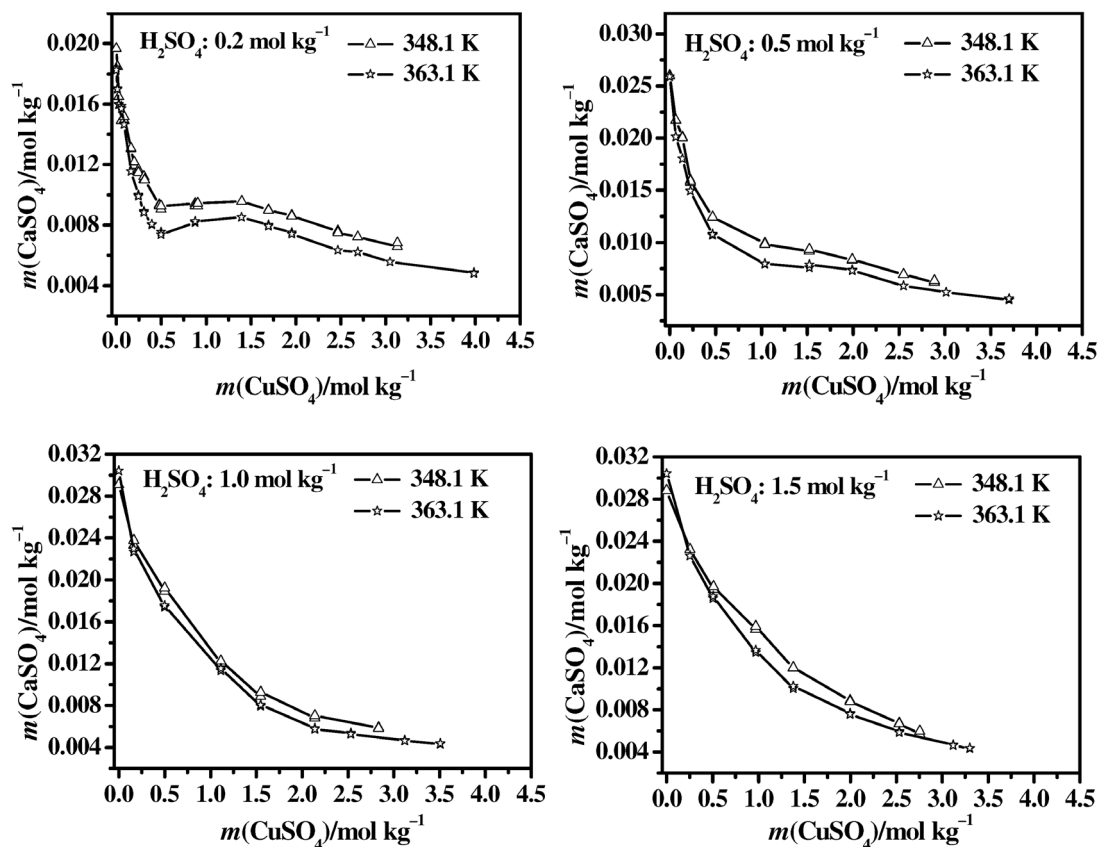

Fig. 21 Temperature influence on the solubility of anhydrite in the $CaSO_4$ + H_2SO_4 + $CuSO_4$ + H_2O system.

Dutrizac and Kuiper [28] reported some solubility data for anhydrite in the $CaSO_4$ + (1.5 mol kg^{-1})H_2SO_4 + (0.5–1.0 mol kg^{-1})$CuSO_4$ + H_2O system over a narrow concentration range. Their data are generally in agreement with our results, with largest relative deviations of 15 % (see Fig. 22). An essential difference is that the solubility of anhydrite in solutions (1.5 mol kg^{-1})H_2SO_4 + (0.5–1.0 mol kg^{-1})$CuSO_4$ decreases with increasing of temperature according to our experimental results, but decreases according to Dutrizac and Kuiper [28], who reported that solid–liquid equilibrium in each case could be reached in 6 h. According to our experimental results, the time needed for equilibrium is at least 4 days.
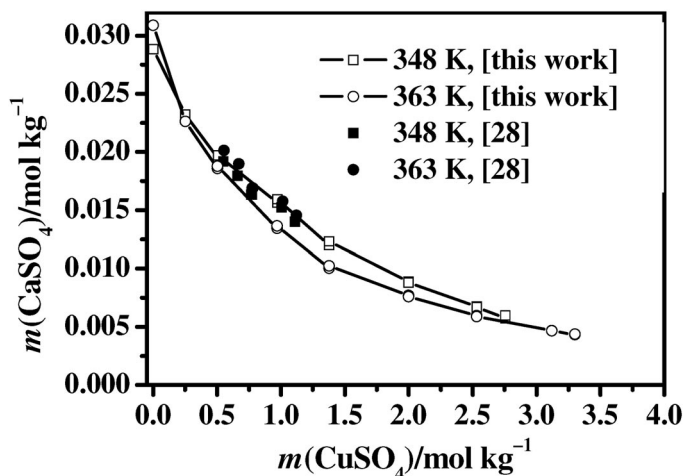

Fig. 22 Solubility of anhydrite in the $CaSO_4$ + (1.5 mol kg^{-1})H_2SO_4 + $CuSO_4$ + H_2O system in this work and comparison with literature data [28].

Farrah et al [34] reported solubility data for anhydrite in the quaternary $CaSO_4$ + H_2SO_4 + $MnSO_4$ + H_2O system, too. We note that their data are generally higher than ours. We also note that Farrah et al's data for anhydrite are generally higher than the predicted values given by Azimi and Papangelakis [37].

INDUSTRIAL SIGNIFICANCE OF THE NEW EXPERIMENTAL DATA

Combining our new experimental data in Figs. 17–19 with the literature data, one can better understand the crystallization behavior of calcium sulfate in hydrometallurgical processes. For example, if $CuSO_4 \cdot 5H_2O$ is used for electroplating, calcium must be controlled to quite a low level (<0.0005 %). Based on the newly obtained results, an effective and simple approach can be developed to avoid the formation of calcium sulfate along with the production of $CuSO_4 \cdot 5H_2O$. In the evaporation-condensation stage of production, if solutions are seeded with anhydrite, calcium sulfate concentration can be decreased to the level A presented in Fig. 23, with an increase of $CuSO_4$ concentration. The anhydrite is then separated at high temperatures. In the following cooling-crystallization stage, the calcium concentration in solution will increase with the crystallization of $CuSO_4 \cdot 5H_2O$ and reach point C in Fig. 23 at 298 K. At this stage, anhydrite does not crystallize, since its solubility increases with increasing temperature. Neither can gypsum form, because the end calcium concentration (expressed by point C in Fig. 23) in the crystallization stage is far lower than the saturated concentration, expressed as point D in Fig. 23. In this way, the formation of calcium sulfate can be avoided in the product, $CuSO_4 \cdot 5H_2O$.

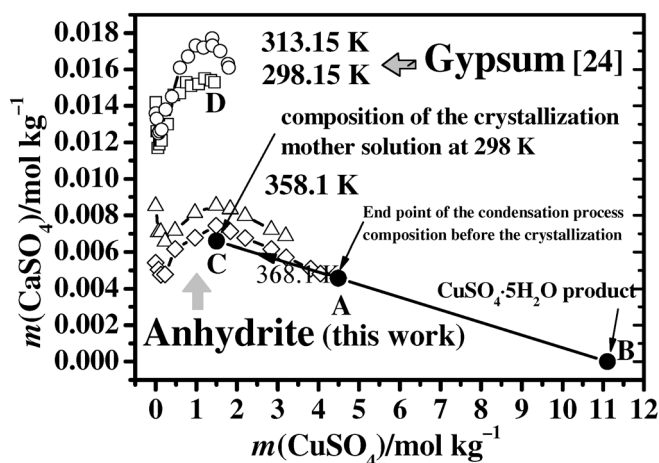**Fig. 23** Solubility changes of $CaSO_4$ in $CuSO_4 \cdot 5H_2O$ production process.

In the hydrometallurgical process to extract zinc, the solubility of calcium sulfate is a function of its hydrate type, temperature, and the concentrations of $ZnSO_4$ and H_2SO_4. The latter three factors change a lot in one process cycle. The temperature changes from about 363 K at the leaching stage to 313 K at the electrowinning stage, and the Zn^{2+} and H_2SO_4 concentrations change from 150 and 0 g L^{-1} in the neutralized leaching solution to about 50 and 200 g L^{-1} in the electrowinning cell, respectively. At the beginning of the leaching stage, the waste electrolyte contains about 50 g L^{-1} Zn^{2+} and 200 g L^{-1} H_2SO_4, and the equilibrium Ca^{2+} concentration with anhydrite is about 0.022 mol kg^{-1} at 363 K, as expressed by point A in Fig. 24. If anhydrite is seeded during the leaching stage, the Ca^{2+} concentration decreases to point B in Fig. 24, at the end of this stage, with Zn^{2+} concentrations increasing and H_2SO_4 concentration decreasing. In the following purification stage when the temperature decreases and Zn^{2+} and H_2SO_4 concentrations are kept approximately constant, anhydrite cannot form since its equilibrium solubility increases with decreasing temperatures (see Fig. 18). Gypsum cannot form because the Ca^{2+} concentration in the electrolyte solution (point B in Fig. 24) is lower than the gypsum
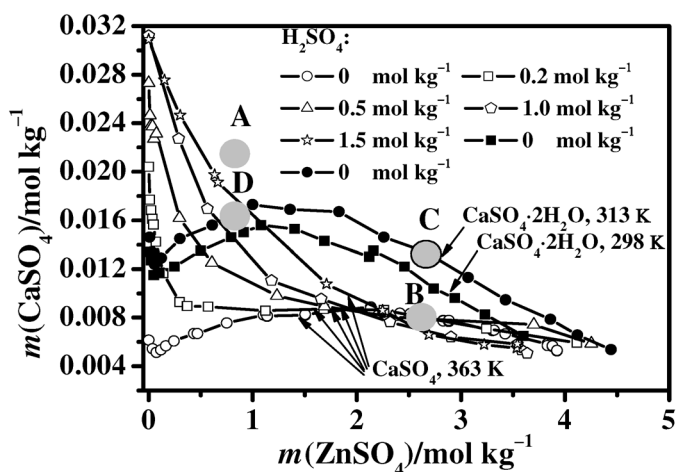

Fig. 24 Solubility changes of $CaSO_4$ in the Zn hydrometallurgical process.

equilibrium concentration (point C in Fig. 24) at temperatures higher than 313 K. In the electrolyte cell where the temperature is about 313 K, the gypsum solubility (point D in Fig. 24) is much higher than the Ca^{2+} concentration in the purified solution (point B in Fig. 24). Based on the process analysis, it is clear that calcium sulfate deposition can be avoided, so long as anhydrite seeding is employed in the leaching stage and crystallization takes place over long enough time.

SUMMARY AND PERSPECTIVE

To avoid the formation of calcium sulfate in hydrometallurgical process involving heavy metals, one must know exactly the solubility behavior of calcium sulfate under the conditions concerned. To this goal, one set of complete solubility phase diagrams for calcium sulfate in the $CaSO_4$ + MSO_4 + H_2SO_4 + H_2O (M: heavy metals) systems is necessary. Up to now, although there has been much investigation of the solubility of calcium sulfate in these systems, most of them have focused on the solubility of gypsum and hemihydrate at relatively lower temperatures. The supplementary investigation in this work on the solubility of anhydrite in these systems helps to better understand the solubility behavior of calcium sulfate at relatively higher temperatures and leads to some novel methods to avoid its formation. However, because of the complexity of the solubility of calcium sulfate, which is a function of hydrate-type, temperature, and concentrations of sulfuric acid and heavy metal sulfate, solubility data for the systems concerned available at present are far from complete.

Thermodynamic modeling of the systems is necessary to obtain one set of complete solubility phase diagrams over a wide range of temperatures and concentrations. For this purpose, a proper thermodynamic model should be selected. For the parameterization of the model, water activities of the MSO_4 + H_2O and MSO_4 + H_2SO_4 + H_2O (M: heavy metals) systems will be quite useful. However, to now, data for these systems are available only at 298 K [38–40]; data at temperatures higher than 298 K need to be determined.

SUPPLEMENTARY INFORMATION

Measured solubility data for anhydrite in the system $CaSO_4$ + H_2SO_4 + MSO_4 + H_2O at 348.1 and 363.1 K are listed in Tables 1–6 in the Supplementary Information for this paper and are available online (doi:10.1351/PAC-CON-10-09-11).

REFERENCES

1. D. Freyer, W. Voigt. *Monatsh. Chem.* **134**, 693 (2003).
2. J. D'Ans, D. Bredtschneider, H. Eick, H. E. Freund. *Kali U. Steinsalz* **9**, 17 (1954).
3. G. A. Hulett. *J. Am. Chem. Soc.* **27**, 49 (1905).
4. G. A. Hulett, L. E. Allen. *J. Am. Chem. Soc.* **24**, 667 (1902).
5. K. U. G. Raju, G. Atkinson. *J. Chem. Eng. Data* **35**, 361 (1990).
6. A. E. Hill. *J. Am. Chem. Soc.* **59**, 2242 (1937).
7. A. C. Melcher. *J. Am. Chem. Soc.* **32**, 50 (1910).
8. E. P. Partridge, A. H. White. *J. Am. Chem. Soc.* **51**, 360 (1929).
9. R. E. Hall, J. A. Robb, C. E. Coleman. *J. Am. Chem. Soc.* **48**, 927 (1926).
10. E. Bock. *Can. J. Chem.* **39**, 1746 (1961).
11. A. E. Hill, J. H. Wills. *J. Am. Chem. Soc.* **60**, 1647 (1938).
12. W. H. Power, B. M. Fabuss. *J. Chem. Eng. Data* **9**, 437 (1964).
13. W. L. Marshall, R. Slusher. *J. Chem. Eng. Data* **13**, 83 (1968).
14. J. Glater, J. Schwartz. *J. Chem. Eng. Data* **21**, 47 (1976).
15. F. K. Cameron, J. F. Breazeale. *J. Phys. Chem.* **7**, 571 (1903).
16. W. L. Marshall, E. V. Jones. *J. Phys. Chem.* **70**, 4028 (1966).

17. A. B. Zdanovskii, G. A. Vlasov. *Russ. J. Inorg. Chem.* **13**, 1318 (1968).
18. J. E. Dutrizac. *Hydrometallurgy* **65**, 109 (2002).
19. A. B. Zdanovskii, G. A. Vlasov. *Russ. J. Inorg. Chem.* **13**, 1418 (1968).
20. Y. Ling, G. P. Demopoulos. *J. Chem. Eng. Data* **49**, 1263 (2004).
21. G. Azimi, V. G. Papangelakis, J. E. Dutrizac. *Fluid Phase Equilib.* **260**, 300 (2007).
22. J. M. Bell, W. C. Taber. *J. Phys. Chem.* **11**, 637 (1907).
23. W. D. Harkins, H. M. Paine. *J. Am. Chem. Soc.* **41**, 1155 (1919).
24. G. Wollmann, W. Vogit. *J. Chem. Eng. Data* **53**, 1375 (2008).
25. B. K. Mutalala, Y. Umetsu, K. Tozawa. *Mater. Trans., JIM* **30**, 394 (1989).
26. Y. Umetsu, B. K. Mutalala, K. Tozawa. *J. Mining Metallurgy Jpn.* **6**, 13 (1989).
27. Y. Umetsu, B. K. Mutalala, K. Tozawa. *Tohoku Daigaku Senko Seiren Kenkyusho Iho* **45**, 13 (1989).
28. J. E. Dutrizac, A. Kuiper. *Hydrometallurgy* **92**, 54 (2008).
29. S. Hagemann. *Entwicklung eines Thermodynamischen Modells fur Zink, Blei und Cadmium insa-linaren Losungen*, p. 219, GRS-report, Braunschweig (2008).
30. V. M. Zatonskaya, N. A. Volkova, S. V. Krashenina, A. I. Samoilenko, N. F. Burtseva. *Tsvetnye Metally (Non-Ferrous Metals)* **29**, 25 (1988).
31. J. E. Dutrizac. *Acta Metall. Slovaca* **65**, 88 (1996).
32. D. M. Korf, E. A. Fomina. *Zh. Neorg. Khim.* **8**, 1022 (1963).
33. B. I. Zhelnin, G. I. Gorshtein, L. K. Bezprozvannaya. *Zh. Prikl. Khim.* **46**, 506 (1973).
34. H. E. Farrah, A. Geoffrey, E. Lawrance, E. J. Wanless. *Hydrometallurgy* **86**, 13 (2007).
35. A. N. Campbell, N. S. Yanick. *Trans. Faraday Soc.* **28**, 657 (1932).
36. G. Azimi, V. G. Papangelakis. *Hydrometallurgy* **102**, 1 (2010).
37. G. Azimi, V. G. Papangelakis. *Fluid Phase Equilib.* **290**, 88 (2010).
38. R. A. Robinson, R. H. Stokes. *Electrolyte Solution*, 2nd ed., 5th revised impression, Butterworths, London (1970).
39. M. Lobo. *Handbook of Electrolyte Solutions*, Elsevier, New York (1989).
40. R. A. Robinson, R. S. Jones. *J. Am. Chem. Soc.* **58**, 959 (1936).